REMOVAL OF ARSENIC ON SORBENTS CONTAINING IRON OXIDE AND TITANIUM OXIDE MODIFIED WITH LANTHANIDE IONS

Sebastian Dudek*, Dorota Kołodyńska

Maria Curie-Skłodowska University
Faculty of Chemistry
Department of Inorganic Chemistry
M. Curie Sklodowska Sq. 2, 20-031 Lublin, Poland

sebastian.dudek@poczta.umcs.lublin.pl

The risk of arsenic compounds

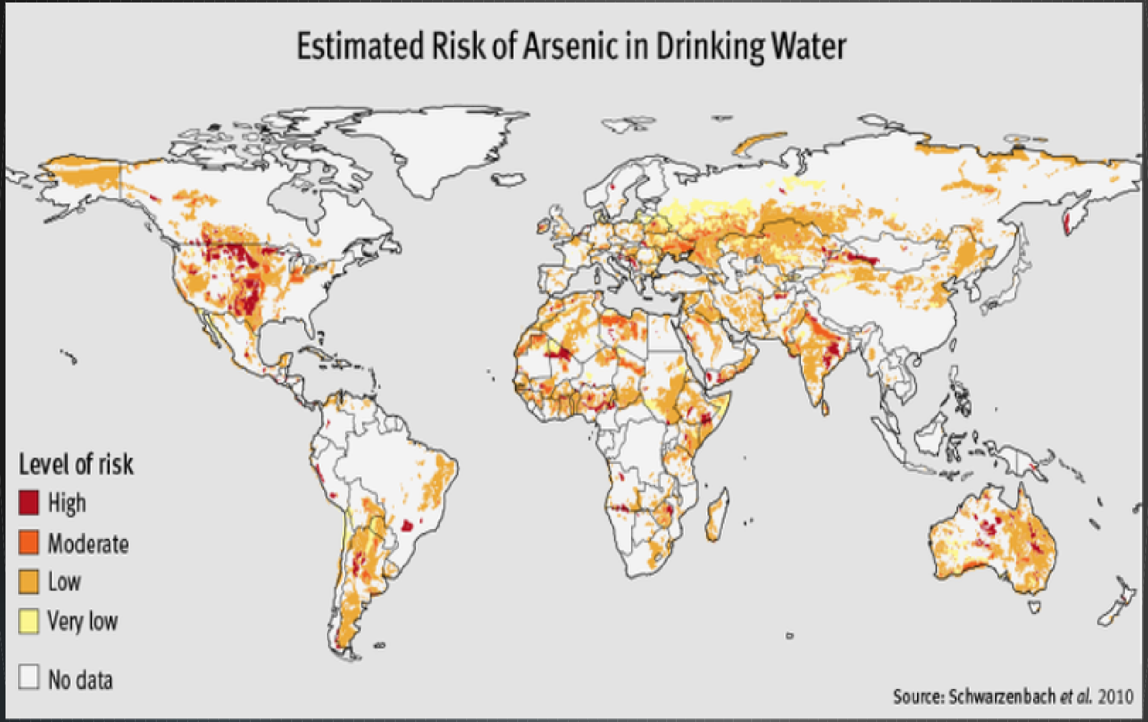

Fig. 1. Estimated risk of arsenic in drinking water.

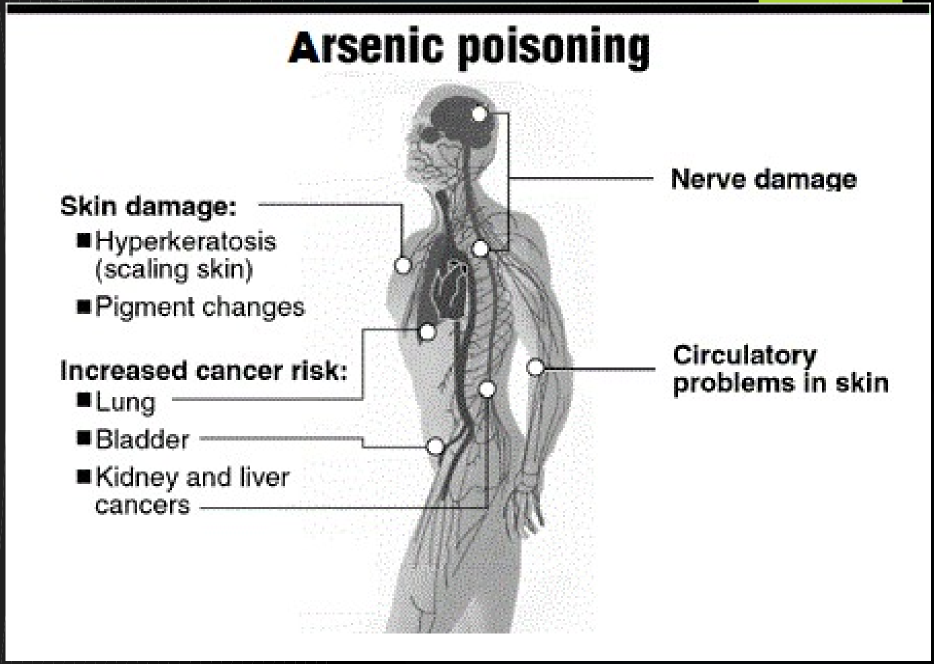

Fig. 2. Effects of arsenic poisoning.

The recommended limit of arsenic concentration in drinkining water
(according to the WHO guidelines):

0.01 mg/L

Sources of arsenic in the environment:

- natural weathering processes,
- volcanic emissions,
- geochemical reactions,
- anthropogenic factors:
  - coal combustion,
  - mining,
  - use of insecticides, herbicides and phosphate fertilizers.

Arsenic chemistry

Arsenic exists mainly in the following oxidation states:

-III +III +V

H_3AsO_3	arsenous acid
H_3AsO_4	arsenic acid
$CH_3AsO_3H_2$	monomethylarsonic acid
$(CH_3)_2AsO_2H$	dimethylarsinic acid aka cacodylic acid
$(CH_3)_3AsO$	trimethylarsine oxide
$(CH_3)_4As^+$	tetramethylarsonium
$(CH_3)_3As^+CH_2CO_2^-$	arsenobetaine
$(CH_3)_3As^+CH_2CH_2OH$	arsenocholine

Fig. 3. Arsenic compounds commonly encountered in environmental materials.

- ❖ Municipal water □ pH 6 to 9
- ❖ Trivalent arsenic is found primarily as H_3AsO_3 which is not ionized
- ❖ Pentavalent arsenic is found primarily as $H_2AsO_4^-$ and $HAsO_4^{2-}$

Toxicity of arsenic compunds:

- ❖ inorganic compounds are more toxic than organic ones
- ❖ As(III) compounds are more toxic than As(V) ones

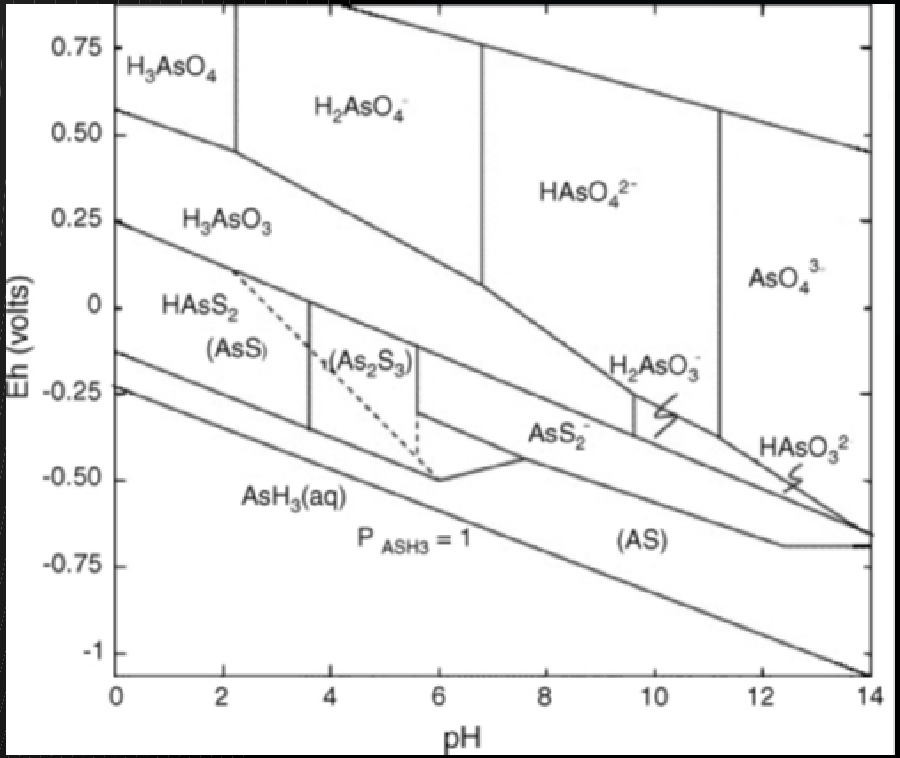

Fig. 4. Species of arsenic in water.

Arsenic removal methods

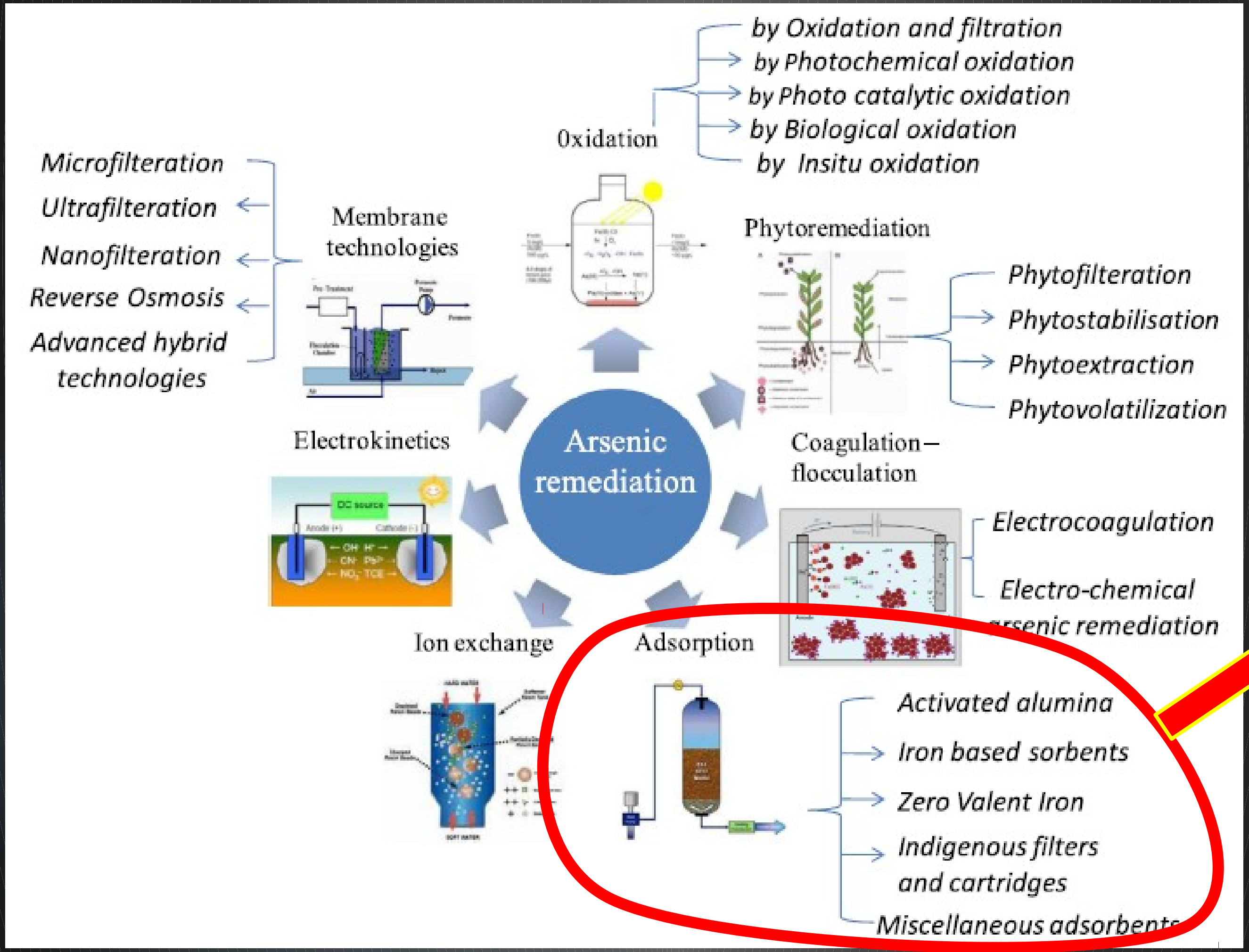

Fig. 5. Examples of arsenic removal methods.

Adsorbents used to remove arsenic should combine the following features:

- high performance,
- low cost
- high durability,
- stable and efficient in changing environmental conditions,
- ability to regenerate.

Sorbent As500

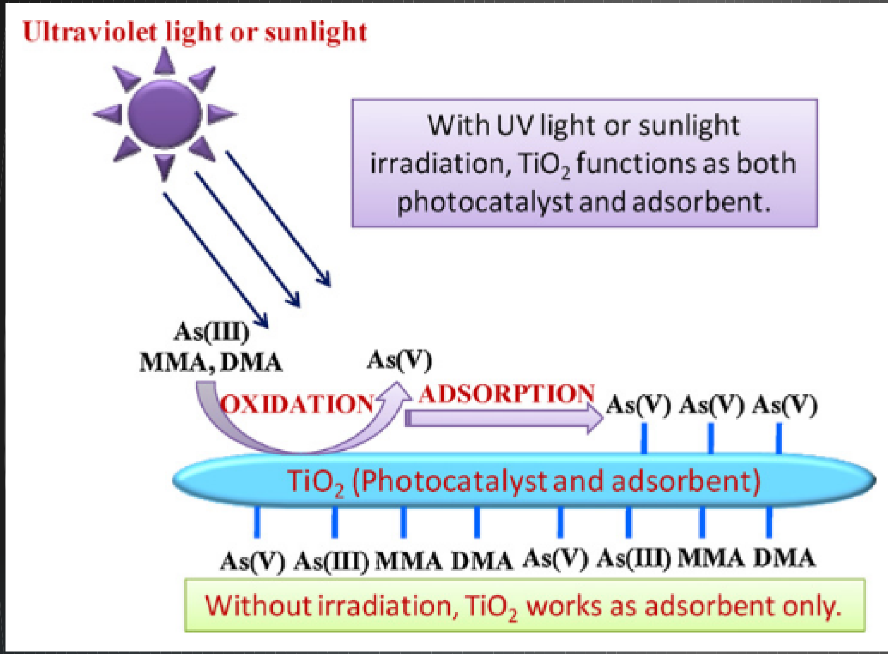

Fig. 6. Schematic illustration of TiO_2 application in arsenic removal.

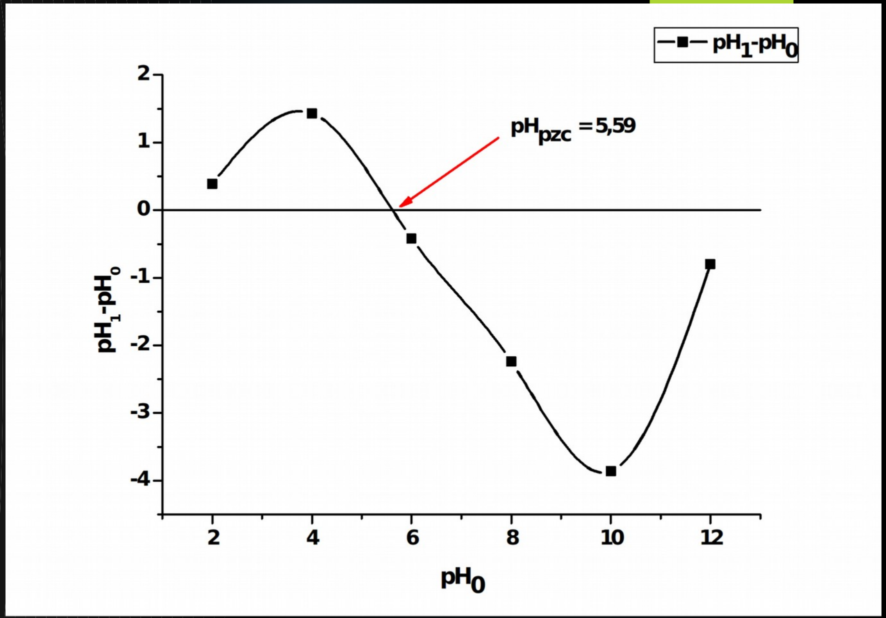

Fig. 7. pH_{pzc} measured by the drift method.

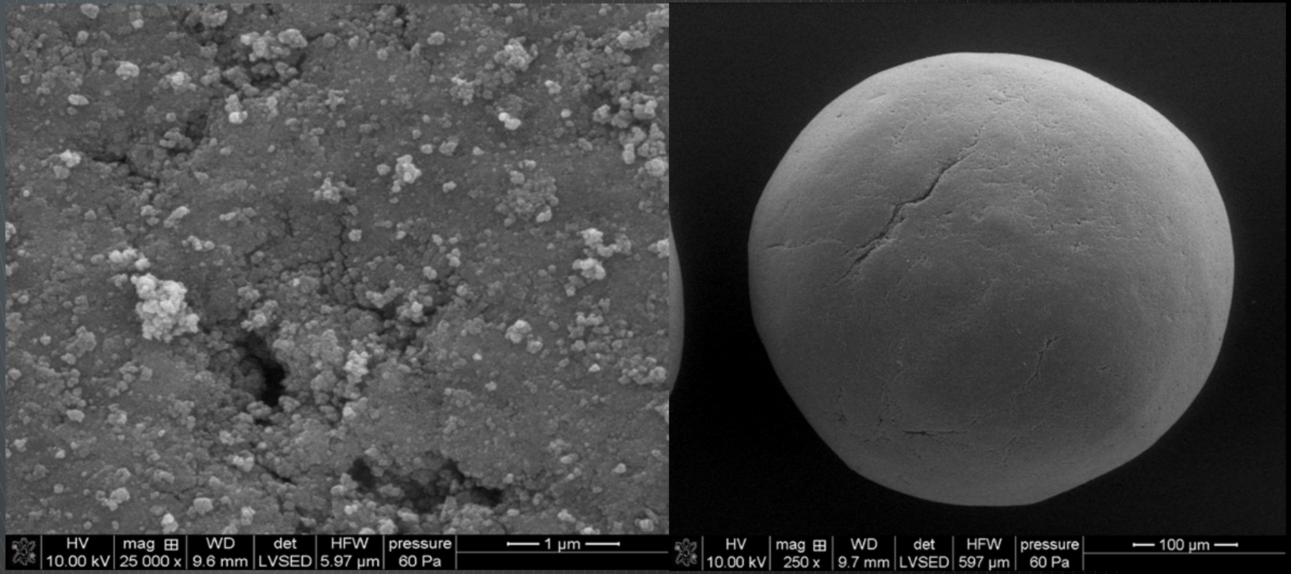

Fig. 8. SEM images of As500.

Sorbent Ferrix A33E

Fig. 9. Ferrix A33E grains

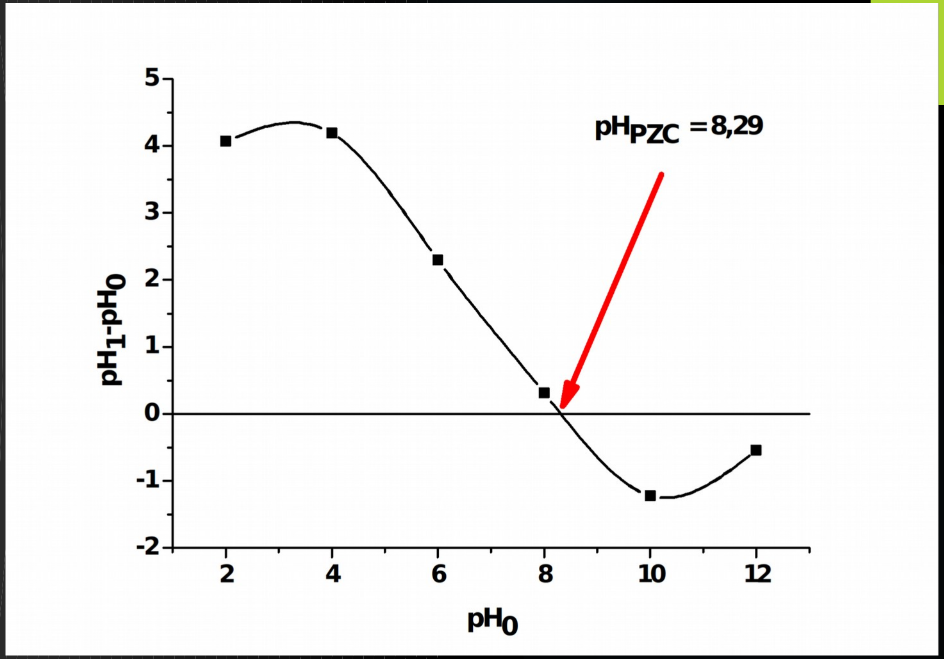

Fig. 10. pH_{pzc} measured by the drift method.

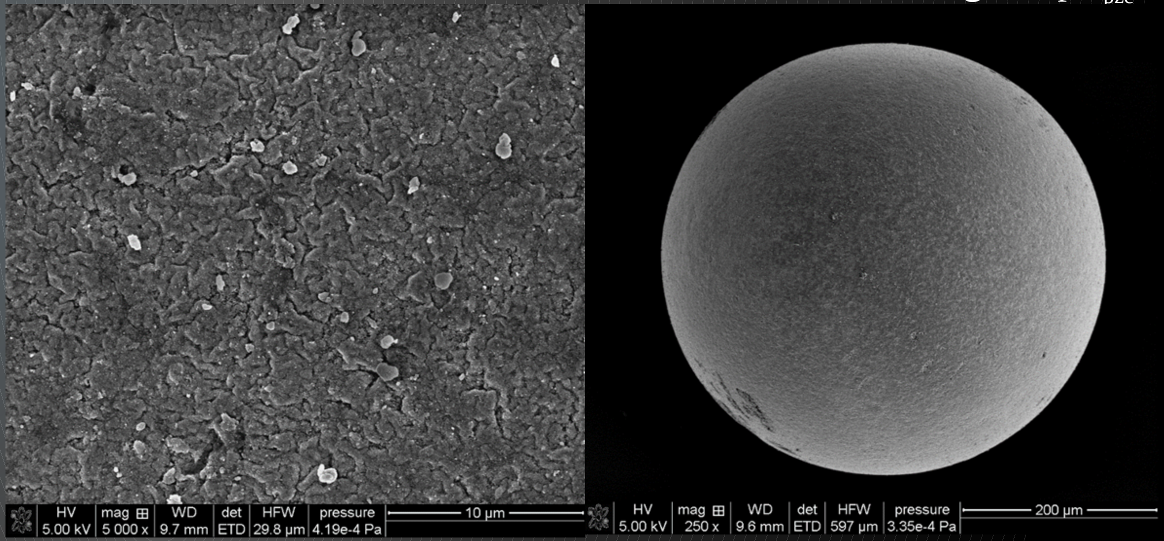

Fig. 11 SEM images of As500.

Main targets

Effectiveness of arsenic sorption on the pure As500 and Ferrix A33E sorbents and with the previously adsorbed lanthanide(III) ions was investigated. The research included:

- determination of adsorption parameters of arsenic ions
- determination of adsorption parameters of lanthanum, neodymium and cerium ions
- comparison of adsorptive properties of the pure As500 and Ferrix A33E sorbents and modified with lanthanide ions towards As(V)

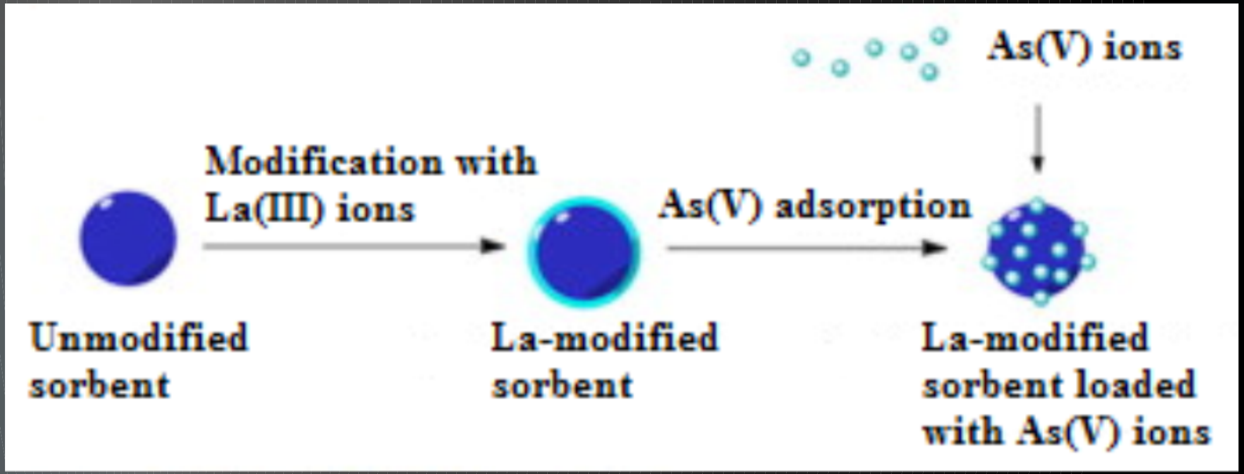

Fig. 13. The scheme of the part of experiment.

Main stages of the study

- effect of pH on the sorption efficiency of As(V) and La(III) ions
- sorption kinetics
- adsorption isotherms
- sorbent selectivity towards lanthanides
- As(V) adsorption on the sorbent with previously adsorbed lanthanide ions

Determination of As(V) and La(III) concentrations

As(V)

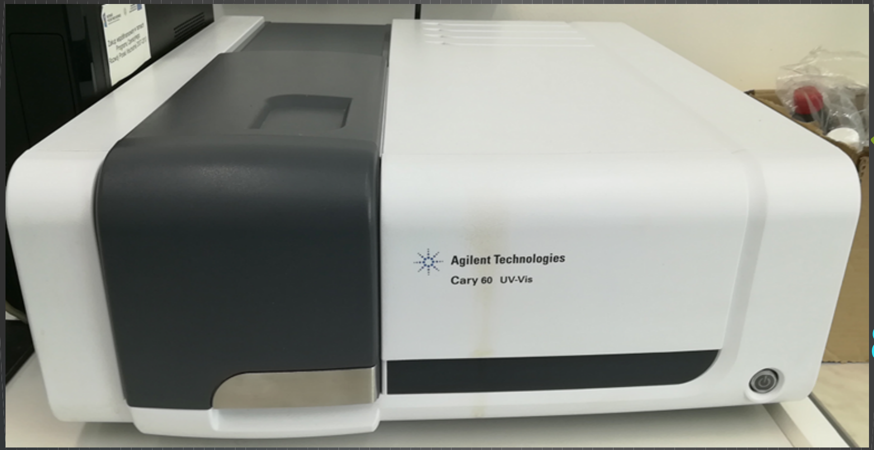

Fig. 10. UV-VIS Spectrophotometer (Cary 60, Agilent Technologies).

870 nm

Concentrations of arsenic(V) ions in the solutions were determined by **UV-VIS spectrophotometry** (Cary 60, Agilent Technologies).

Fig. 12. The solutions of arsenic complex compunds prepared to determine the standard curve.

La(III)

Fig. 11. Inductively Coupled Plasma-Optical Emission Spectrometer ICP-OES (720-Es, Varian).

Concentrations of lanthanide(III) ions in the solutions were determined by **Inductively Coupled Plasma Optical Emission Spectrometry** (ICP-OES, 720-ES, Varian)

The **amount of adsorbed metal** (*qt*) was estimated from the following relation:

$$q_t = (c_0 - c_t) \times \frac{V}{m}$$

where q_t is the amount of adsorbed metal (mg/g), c_0 is the initial concentration of metal in the solution (mg/L), c_t is the concentration of metal in the solution after time t (mg/L), V is the volume of the solution containing metal ions (L), m is the mass of sorbent (g).

where q_t is the amount of adsorbed metal (mg/g), c_0 is the initial concentration of metal in the solution (mg/L), c_t is the concentration of metal in the solution after time t (mg/L), V is the volume of the solution containing metal ions (L), m is the mass of sorbent (g).

The percentage of adsorption (%S) is that of metal adsorbed on the adsorbent beads calculated by the following equation:

$$\%S = (c_0 - c_t)/c_0 \times 100\%$$

Kinetic parameters of metal ions sorption onto the sorbent were determined using the following equations:

$$log(q_e - q_t) = log(q_e) - \frac{k_1}{2,303} \times t$$

$$\frac{t}{q_t} = \frac{1}{k_2 \times q_2^2} + \frac{1}{q_2} \times t$$

where *qe* is the mass of adsorbed metal ions at equilibrium (mg/g), *qt* is the mass of adsorbed metal ions at time *t* (mg/g), k_1 and k_2 are the reaction rate constants of the pseudo-first order (1/min) and pseudo-second order (g/mg min)

where *qe* is the mass of adsorbed metal ions at equilibrium (mg/g), *qt* is the mass of adsorbed metal ions at time *t* (mg/g), k_1 and k_2 are the reaction rate constants of the pseudo-first order (1/min) and pseudo-second order (g/mg min)

Adsorption isotherms were determined from the equations:

Langmuir model $$q_e = \frac{q_0 K_L c_e}{1 + K_L c_e}$$

Freundlich model $$q_e = K_F c_e^{1/n}$$

where:

q_o- the maximum adsorption capacity (mg/g)

K_L- the Langmuir coefficient (dm^3/mg)

K_F- roughly an indicator of the adsorption capacity (mg/g)

n- empirical parameter; the heterogeneity factor

Effect of pH on As(V) removal efficiency

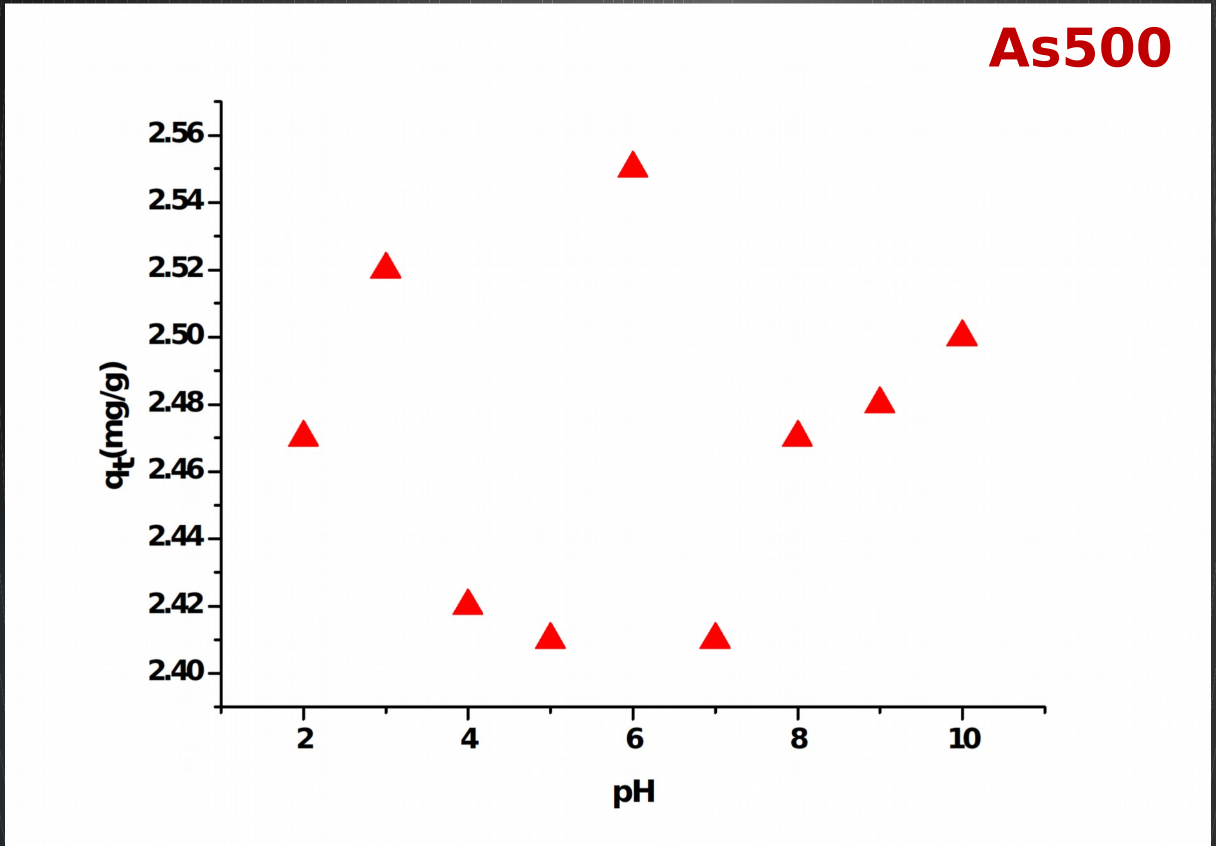

Fig. 14. Effect of pH on As(V) ions removal efficiency (As500, c = 10 mg/dm^3, m = 0,1 g, t = 24 h).

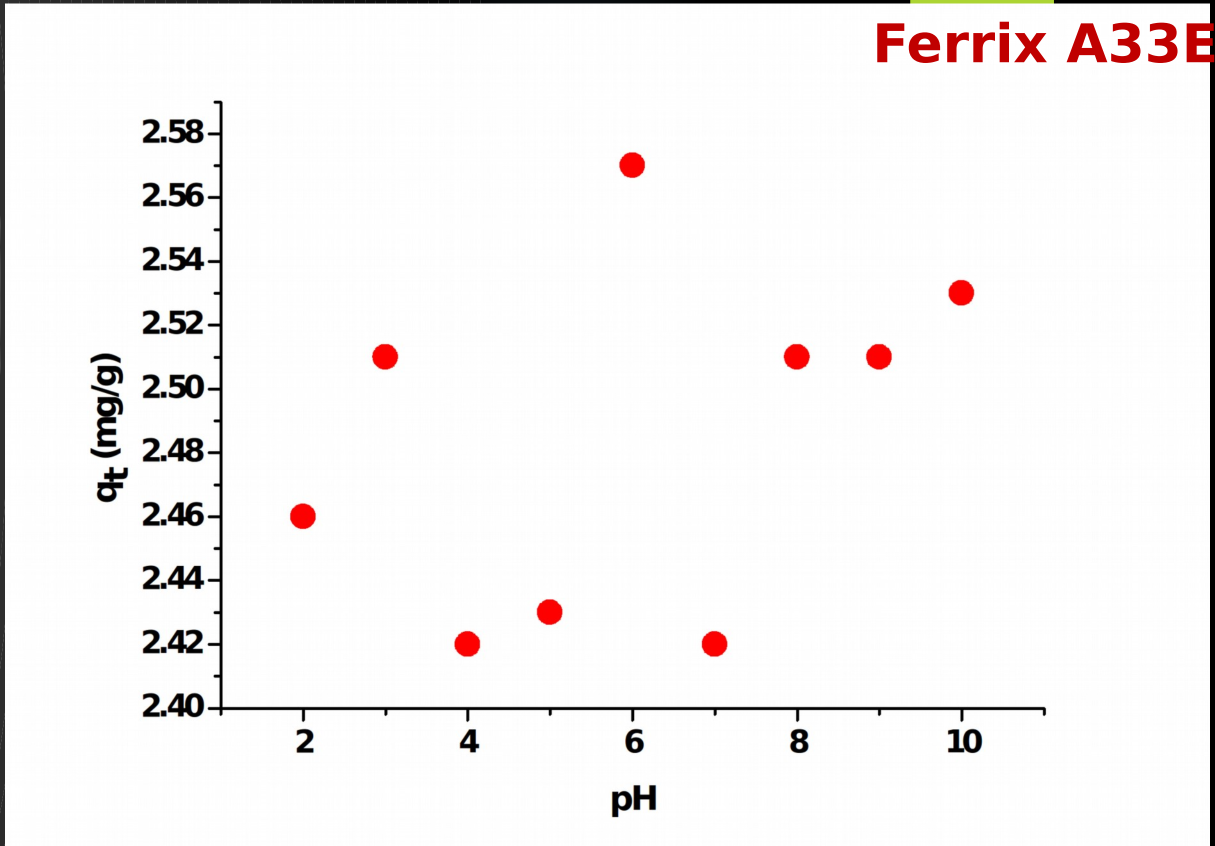

Fig. 15. Effect of pH on As(V) ions removal efficiency (Ferrix A33E, c = 10 mg/dm^3, m = 0,1 g, t = 24 h).

The maximum sorption capacity towards As(V) ions was achieved at **pH 6**.

Effect of pH on adsorption efficiency of La(III) ions as model ions for other lanthanides

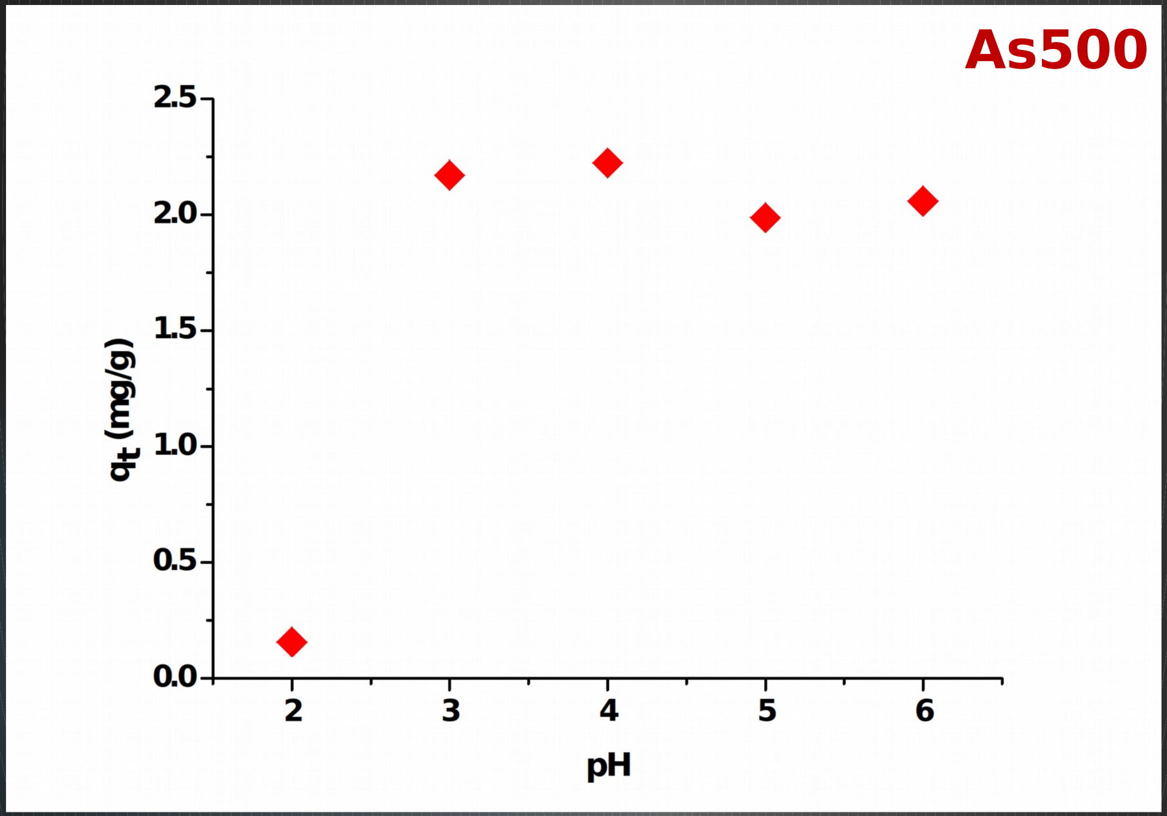

Fig. 16. Effect of pH on La ions removal efficiency (As500, c = 10 mg/dm^3, m = 0,1 g, t = 24 h).

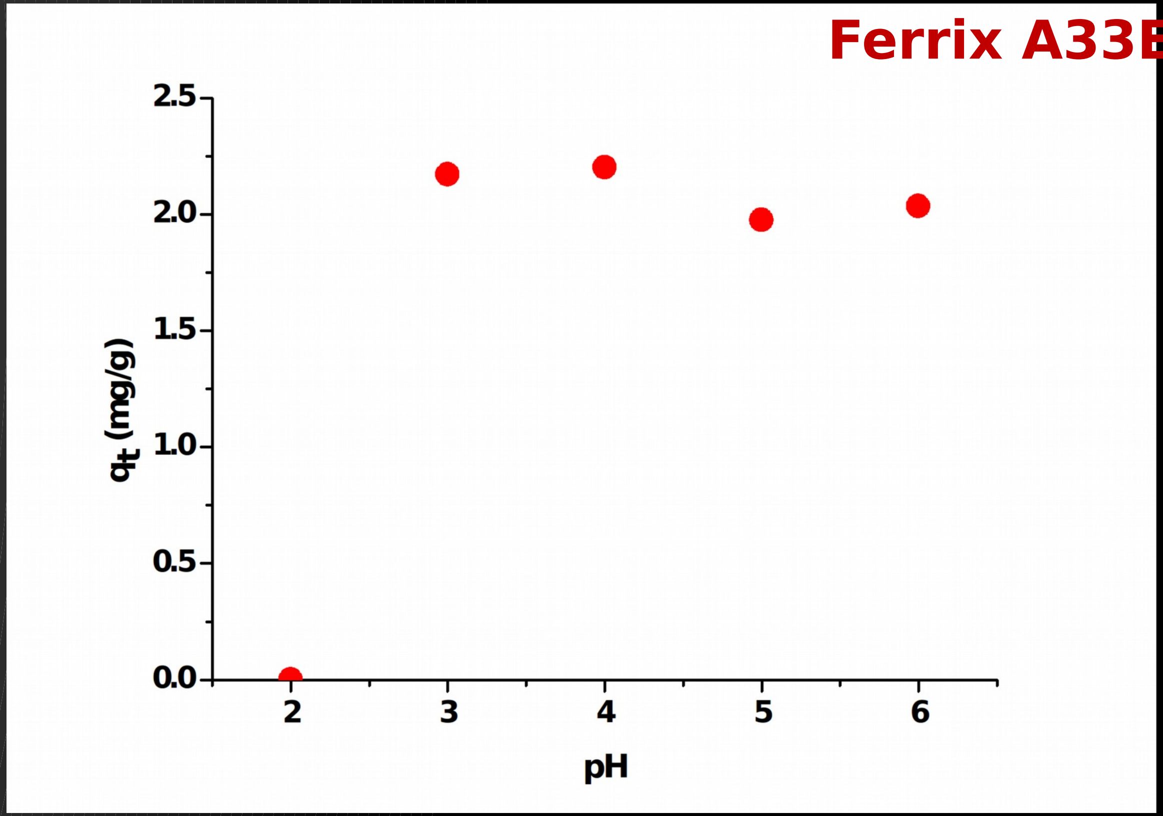

Fig. 17. Effect of pH on La ions removal efficiency (Ferrix A33E, c = 10 mg/dm^3, m = 0,1 g, t = 24 h).

The maximum sorption capacity towards La(III) ions was achieved at pH 4.

Effect of contact time and initial concentration of As(V) on the adsorption efficiency

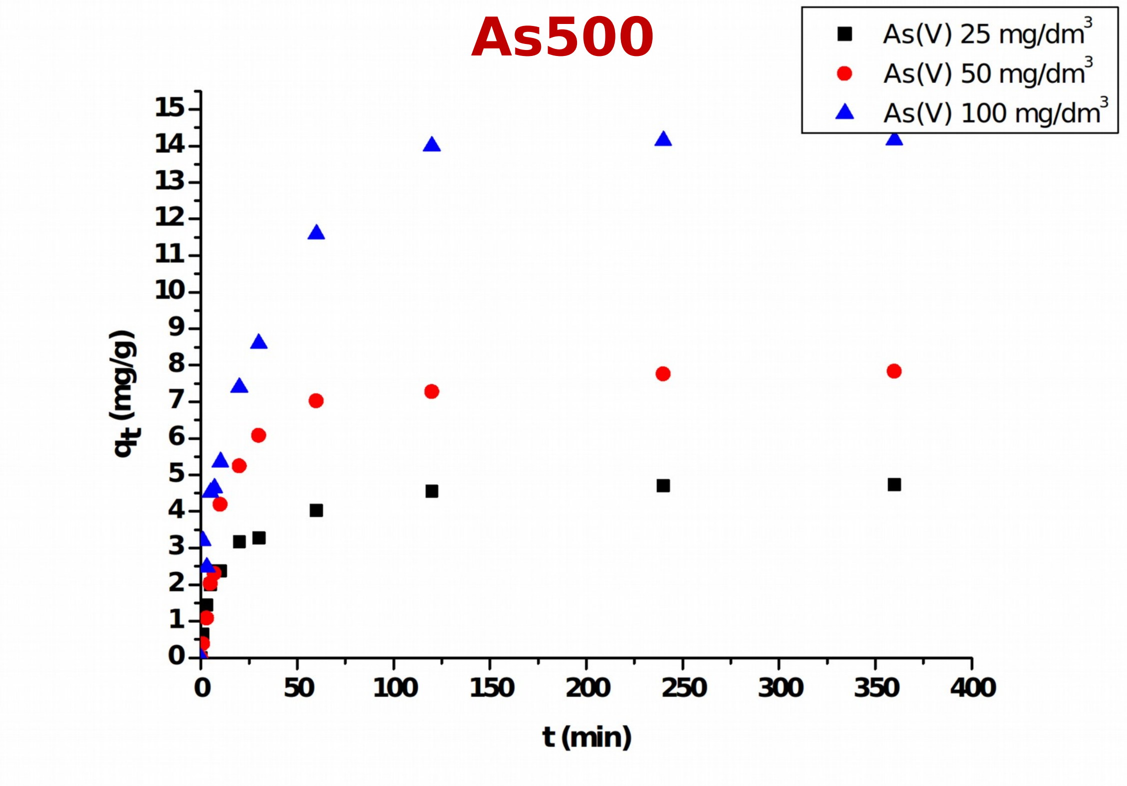

Fig. 18. Graph of the sorption capacities of the adsorbent as a function of time at As(V) initial concentrations equal to 25, 50 and 100 mg/dm³.

Kinetic parameters	As(V)-As500		
	25 [mg/dm³]	50 [mg/dm³]	100 [mg/dm³]
Pseudo-first order model			
q_1 [mg/g]	4.74	7.83	15.56
$q_{1.cal}$ [mg/g]	2.61	4.25	10.69
k_1 [1/min]	0.046	0.037	0.034
R^2	0.8172	0.5433	0.8202
Pseudo-second order model			
q_2 [mg/g]	4.74	7.83	15.56
$q_{2.cal}$ [mg/g]	3.15	5.28	10.53
k_2 [g/g·min]	0.021	0.010	0.005
h [mg/min]	0.211	0.293	0.506
R^2	0.9724	0.9989	0.9973

Fig. 19. Determined kinetic parameters of the As(V) adsorption process on the tested sorbent.

Effect of contact time and initial concentration of As(V) on the adsorption efficiency

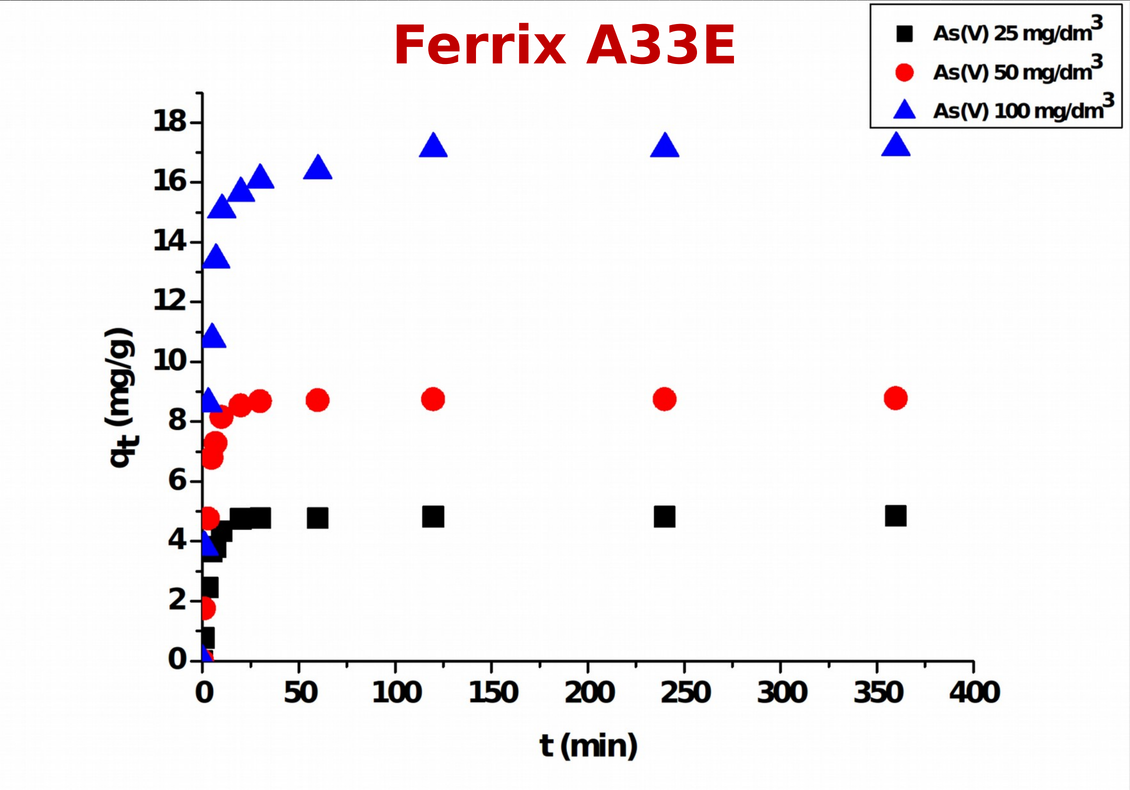

Fig. 20. Graph of the sorption capacities of the adsorbent as a function of time at As(V) initial concentrations equal to 25, 50 and 100 mg/dm³.

Kinetic parameters	As(V)-Ferrix A33E		
	25 [mg/dm³]	**50 [mg/dm³]**	**100 [mg/dm³]**
Pseudo-first order model			
q_1 [mg/g]	4.84	8.78	17.16
$q_{1.cal}$ [mg/g]	0.65	1.05	4.30
k_1 [1/min]	0.018	0.019	0.027
R^2	0.5226	0.5502	0.8162
Pseudo-second order model			
q_2 [mg/g]	4.84	8.78	17.16
$q_{2.cal}$ [mg/g]	4.87	8.82	17.30
k_2 [g/g·min]	0.105	0.073	0.023
h [mg/min]	2.482	5.648	6.990
R^2	0.9999	0.9999	1.0000

Fig. 21. Determined kinetic parameters of the As(V) adsorption process on the tested sorbent.

Effect of contact time and initial concentration of lanthanides(III) on the adsorption efficiency

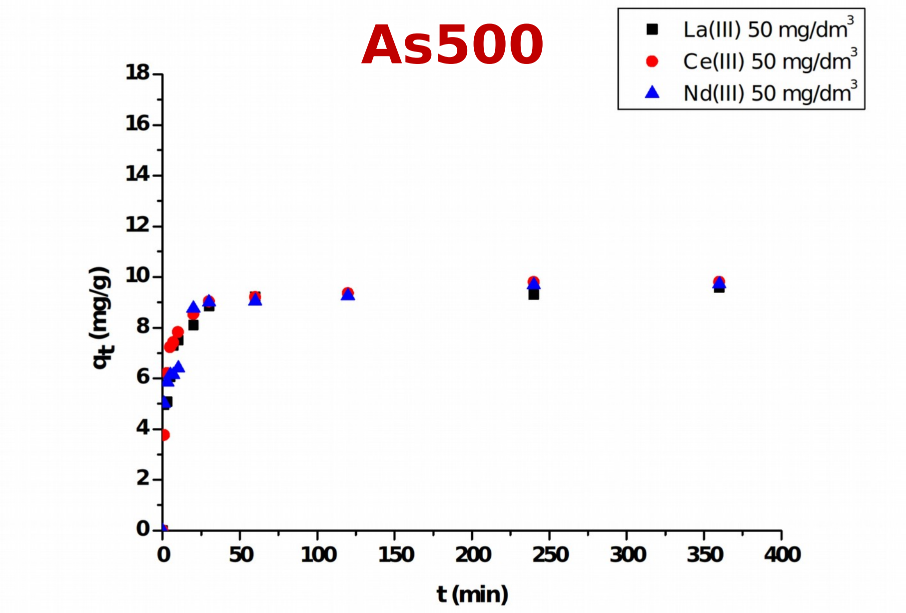

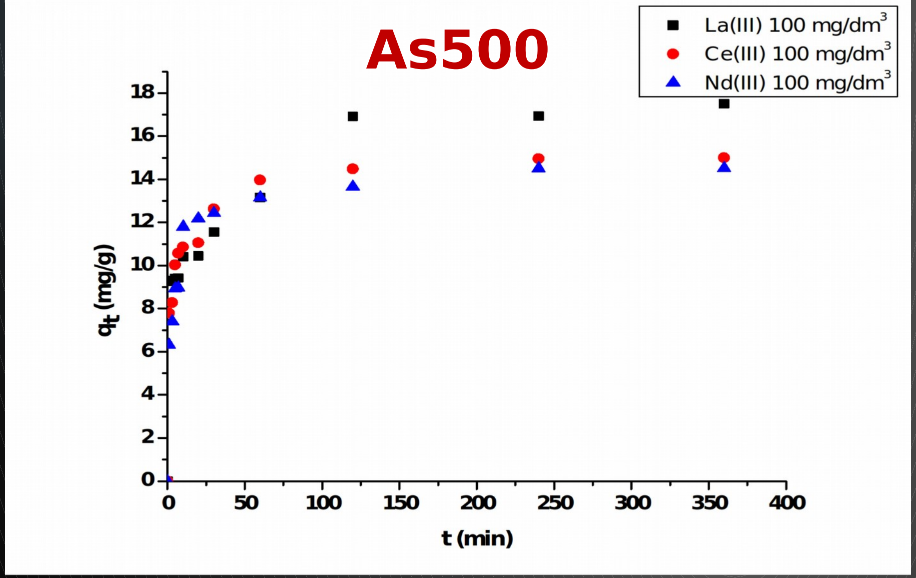

Fig. 22. Graphs of the sorption capacities of As500 as a function of time at La(III), Ce(III), Nd(III) initial concentrations equal to 50 and 100 mg /dm^3.

Fig. 23. Graphs of the sorption capacities of Ferrix A33E as a function of time at La(III), Ce(III), Nd(III) initial concentrations equal to 50 and 100 mg /dm^3.

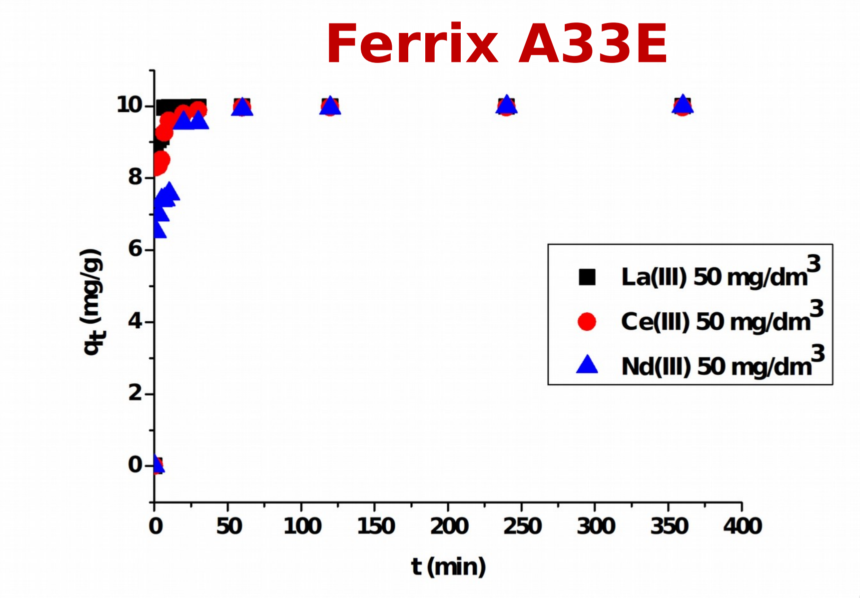

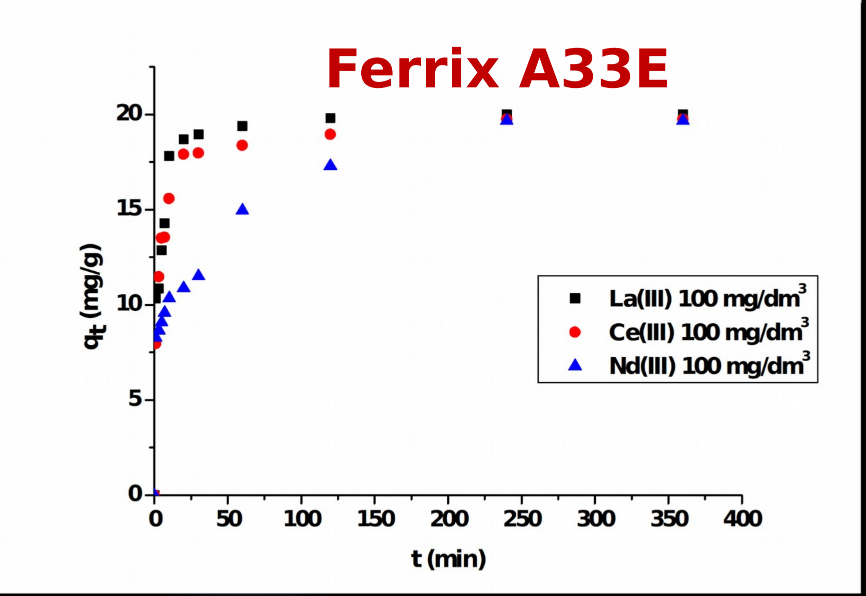

Effect of contact time and initial concentration of lanthanides(III) on the adsorption efficiency

Kinetic parameters	La(III)-As500		
	10 [mg/dm^3]	50 [mg/dm^3]	100 [mg/dm^3]
Pseudo-first order model			
q_1 [mg/g]	2.00	9.57	17.51
$q_{1.cal}$ [mg/g]	0.11	2.26	8.10
k_1 [1/min]	0.025	0.012	0.013
R^2	0.6012	0.6378	0.8630
Pseudo-second order model			
q_2 [mg/g]	2.00	9.57	17.51
$q_{2.cal}$ [mg/g]	2.00	9.57	17.74
k_2 [g/g·min]	0.983	0.039	0.007
h [mg/min]	3.930	3.533	2.068
R^2	0.9999	0.9998	0.9973

Kinetic parameters	Ce(III)-As500		
	50 [mg/dm^3]	75 [mg/dm^3]	100 [mg/dm^3]
Pseudo-first order model			
q_1 [mg/g]	9.80	11.89	15.00
$q_{1.cal}$ [mg/g]	3.16	4.64	5.50
k_1 [1/min]	0.025	0.025	0.020
R^2	0.9310	0.9439	0.9807
Pseudo-second order model			
q_2 [mg/g]	9.80	11.89	15.00
$q_{2.cal}$ [mg/g]	9.86	12.05	15.15
k_2 [g/g·min]	0.037	0.020	0.017
h [mg/min]	3.567	2.868	3.819
R^2	0.9998	0.9997	0.9998

Kinetic parameters	Ce(III)-Ferrix A33E		
	50 [mg/dm^3]	75 [mg/dm^3]	100 [mg/dm^3]
Pseudo-first order model			
q_1 [mg/g]	9.96	14.98	19.74
$q_{1.cal}$ [mg/g]	0.65	4.11	7.30
k_1 [1/min]	0.037	0.033	0.029
R^2	0.8817	0.7496	0.9322
Pseudo-second order model			
q_2 [mg/g]	9.96	14.98	19.74
$q_{2.cal}$ [mg/g]	9.98	15.17	19.88
k_2 [g/g·min]	0.236	0.019	0.017
h [mg/min]	23.508	4.328	6.681
R^2	1.0000	0.9996	0.9999

Kinetic parameters	Nd(III)-As500		
	50 [mg/dm^3]	75 [mg/dm^3]	100 [mg/dm^3]
Pseudo-first order model			
q_1 [mg/g]	9.73	11.84	14.53
$q_{1.cal}$ [mg/g]	3.00	4.83	5.83
k_1 [1/min]	0.018	0.018	0.023
R^2	0.8852	0.9360	0.9428
Pseudo-second order model			
q_2 [mg/g]	9.73	11.84	14.53
$q_{2.cal}$ [mg/g]	9.80	11.94	14.65
k_2 [g/g·min]	0.030	0.016	0.017
h [mg/min]	2.865	2.334	3.600
R^2	0.9998	0.9992	0.9997

Kinetic parameters	La(III)-Ferrix A33E		
	10 [mg/dm^3]	50 [mg/dm^3]	100 [mg/dm^3]
Pseudo-first order model			
q_1 [mg/g]	2.00	10.00	20.00
$q_{1.cal}$ [mg/g]	0.03	0.14	5.09
k_1 [1/min]	0.016	0.016	0.028
R^2	0.3757	0.3757	0.9344
Pseudo-second order model			
q_2 [mg/g]	2.00	10.00	20.00
$q_{2.cal}$ [mg/g]	2.00	10.00	20.12
k_2 [g/g·min]	3.113	0.623	0.025
h [mg/min]	12.454	62.270	10.010
R^2	1.0000	1.0000	1.0000

Kinetic parameters	Nd(III)-Ferrix A33E		
	50 [mg/dm^3]	75 [mg/dm^3]	100 [mg/dm^3]
Pseudo-first order model			
q_1 [mg/g]	9.99	14.89	19.67
$q_{1.cal}$ [mg/g]	1.80	10.32	15.93
k_1 [1/min]	0.026	0.023	0.029
R^2	0.8482	0.9533	0.9175
Pseudo-second order model			
q_2 [mg/g]	9.99	14.89	19.67
$q_{2.cal}$ [mg/g]	10.04	15.27	20.18
k_2 [g/g·min]	0.063	0.006	0.004
h [mg/min]	6.334	1.352	1.773
R^2	1.0000	0.9954	0.9961

Fig. 24. Determined kinetic parameters of the adsorption processes of La(III), Ce(III) and Nd(III).

Parameters of adsorption isotherms

Table 1
The Langmuir and Freundlich parameters for adsorption of arsenic(V) and lanthanides(III) on As500.

Ion	Adsorption model					
	Langmuir			Freundlich		
	q_m	b	R^2	n	K_F	R^2
As(V)	36.70	0.033	0.9862	2.534	3.91	0.9502
La(III)	19.29	0.620	0.9999	4.265	6.40	0.8947
Nd(III)	13.34	0.270	0.9997	19.114	9.79	0.9463
Ce(III)	15.91	0.399	0.9999	11.945	10.13	0.8587

Table 2
The Langmuir and Freundlich parameters for adsorption of arsenic(V) and lanthanides(III) on Ferrix A33E.

Ion	Adsorption model					
	Langmuir			Freundlich		
	q_m	b	R^2	n	K_F	R^2
As(V)	35.96	0.081	0.9963	2.841	5.77	0.8635
La(III)	58.95	6.439	1.0000	4.087	24.60	0.6232
Nd(III)	39.52	0.585	0.9994	6.558	18.40	0.8435
Ce(III)	60.57	0.985	1.0000	4.425	23.26	0.7432

Table 3
Comparison of the different sorbents based on oxides for arsenic removal.

Adsorbent type	pH	Maximum adsorption capacity [mg/g]	Authors
$Fe_3O_4@SiO_2@TiO_2$ nanosorbent	9.0	10.2	(Feng et al., 2017)
Mg doped α-Fe_2O_3	7.0	10	(Tang et al., 2013)
Fe_3O_4	8.2	12.56	(Akin et al., 2012)
Nanoscale zero-valent iron-reduce graphite oxide modified composite	7.0	29.04	(Wang et al., 2014)
Hydrated ferric hydroxide	9.0	7.0	(Lenoble et al., 2002)
As500	**6.0**	**36.70**	-
Ferrix A33E	**6.0**	**35.96**	-

Selectivity

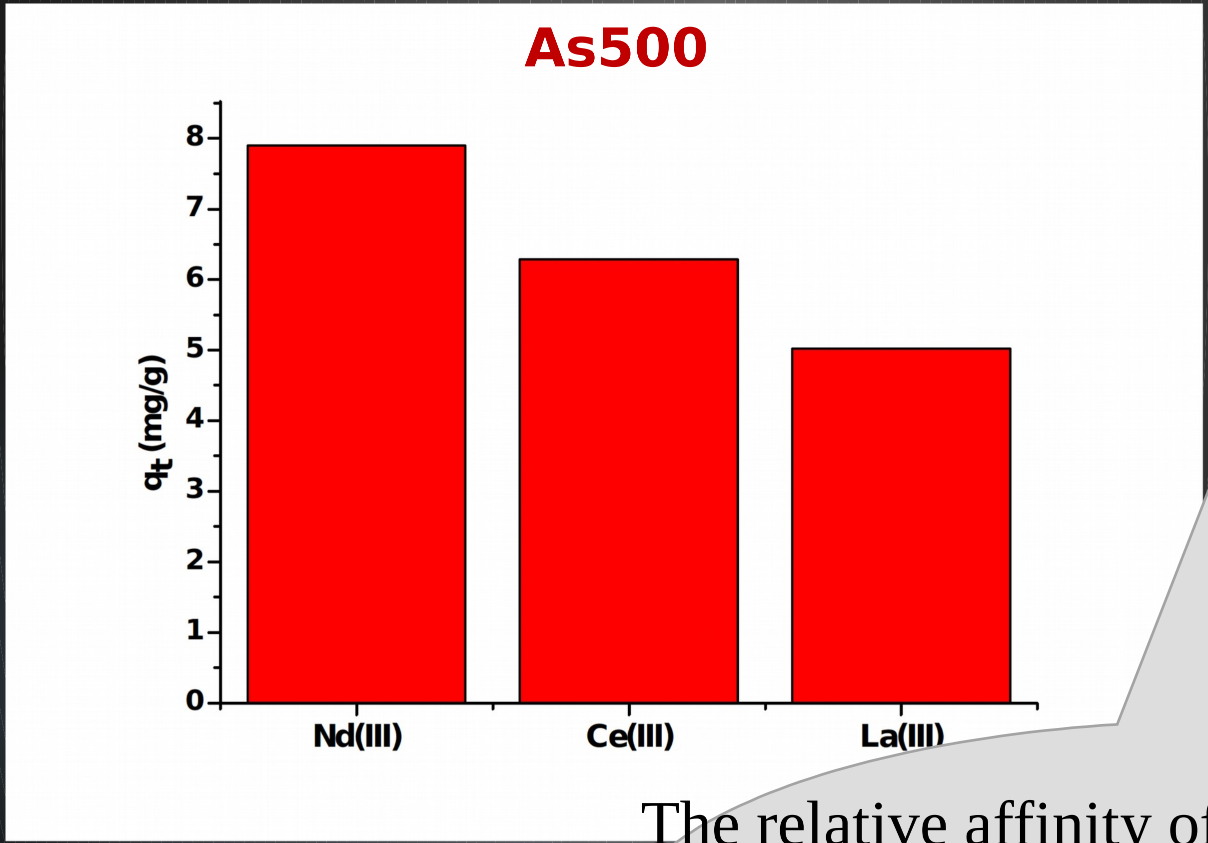

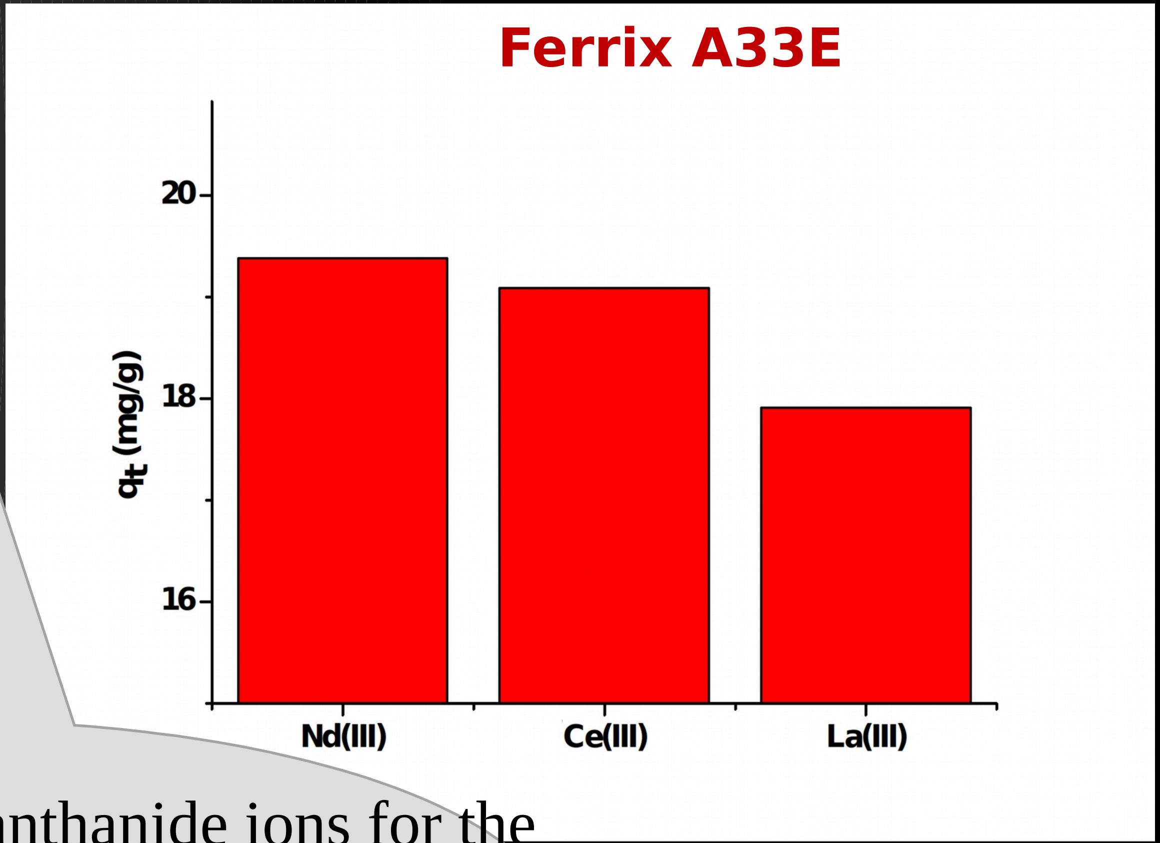

The relative affinity of lanthanide ions for the sorbents:

Nd(III) > Ce(III) > La(III)

Fig. 25. Graph of the sorption effic… lanthanide ions from the mixture (conce… equal to 100 mg/…

…iciency in the case of adsorption of …ncentration of La(III), Nd(III) and Ce(III) … mg/L (Ferrix A33E).

Adsorption of arsenic on the sorbent modified with lanthanide ions

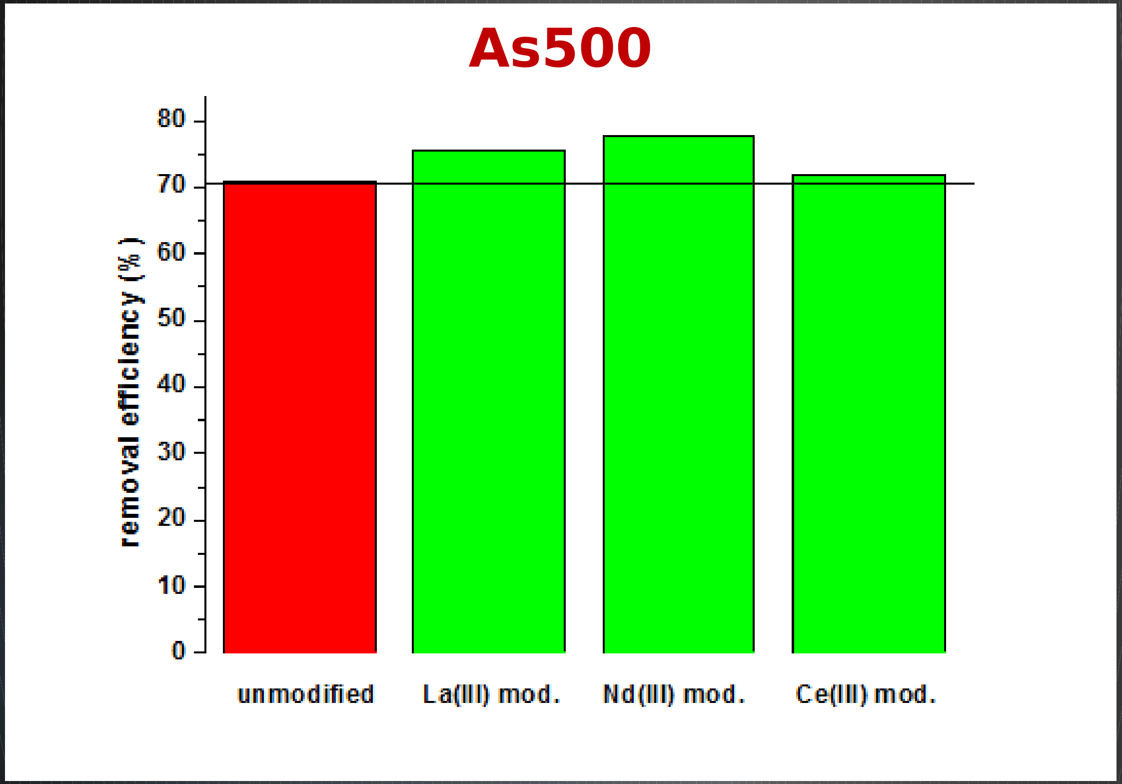

Fig. 26. Enhanced arsenic adsorption caused by modification of As500 with lanthanide ions (As500, c_{As} = 100 mg/dm^3, m = 0,1 g, t = 6 h).

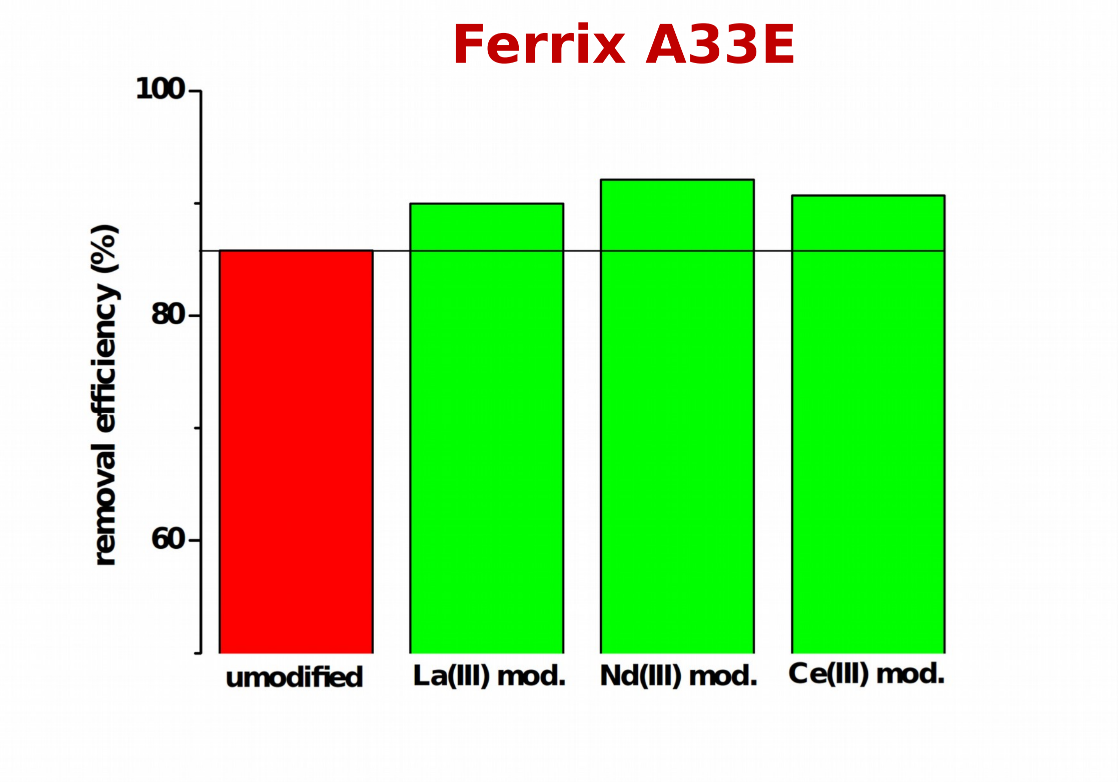

Fig. 27. Enhanced arsenic adsorption caused by modification of Ferrix A33E with lanthanide ions (Ferrix A33E, c_{As} = 100 mg/dm^3, m = 0,1 g, t = 6 h) .

Conclusions

- The equilibrium of arsenic and lanthanide adsorption is achieved relatively quickly.
-

As500

Ion	Adsorption model					
	Langmuir			Freundlich		
	q_m	b	R^2	n	K_F	R^2
As(V)	36.70	0.033	0.9862	2.534	3.91	0.9502
La(III)	19.29	0.620	0.9999	4.265	6.40	0.8947
Nd(III)	13.34	0.270	0.9997	19.114	9.79	0.9463
Ce(III)	15.91	0.399	0.9999	11.945	10.13	0.8587

Ferrix A33E

Ion	Adsorption model					
	Langmuir			Freundlich		
	q_m	b	R^2	n	K_F	R^2
As(V)	35.96	0.081	0.9963	2.841	5.77	0.8635
La(III)	58.95	6.439	1.0000	4.087	24.60	0.6232
Nd(III)	39.52	0.585	0.9994	6.558	18.40	0.8435
Ce(III)	60.57	0.985	1.0000	4.425	23.26	0.7432

As500:
sorption capacity towards
As(V) → 36.70 mg/g

Ferrix A33E:
sorption capacity towards
As(V) → 35.96 mg/g

Ferrix A33E has much larger sorption capacities towards lanthanide ions than As500

After sorption of lanthanides the sorption capacities are even greater!
The highest increase of about 7 percentage points:
Nd(III) modification
As500:
~~85,8%~~ → **92,09%**
Ferrix A33E
~~70,8%~~ → **77,70%**

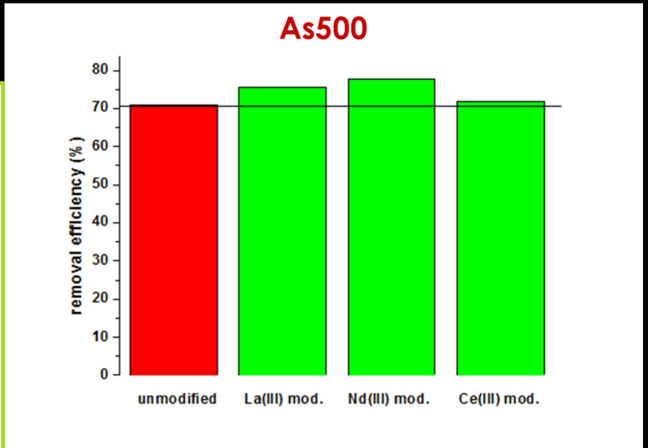

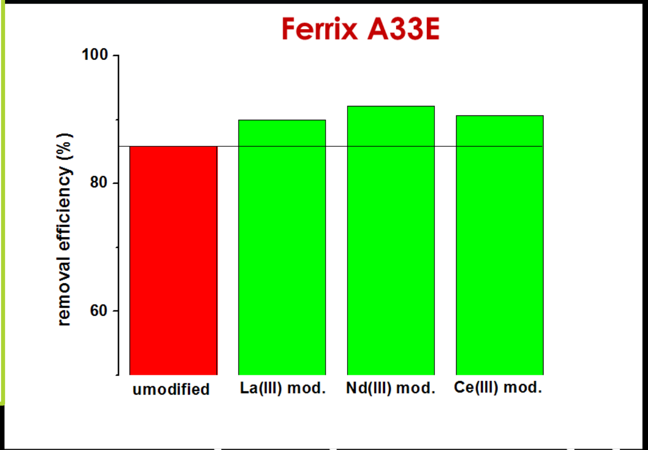

- Preeliminary results are very promising but much more research to optimize the process and regenerate the sorbents is needed.
- This process can contribute to a significant reduction in the amount of arsenic in the environment.

References:

1. Ng, J.C.; Wang, J.; Shraim, A. A global health problem caused by arsenic from natural sources. *Chemosphere* **2003**, *52*, 1353–1359.
2. Kartinen, E.O.; Martin, C.J. An overview of arsenic removal processes. *Desalination* **1995**, *103*, 79–88.
3. Bissen, M.; Vieillard-Baron, M.M.; Schindelin, A.J.; Frimmel, F.H. TiO2-catalyzed photooxidation of arsenite to arsenate in aqueous samples. *Chemosphere* **2001**, *44*, 751–757.
4. Feng, C.; Aldrich, C.; Eksteen, J.J.; Arrigan, D.W.M. Removal of arsenic from alkaline process waters of gold cyanidation by use of γ-Fe_2O_3@ZrO_2 nanosorbents. *Hydrometallurgy* **2017**, *174*, 71–77.
5. Tang, W.; Su, Y.; Li, Q.; Gao, S.; Shang, J.K. Mg-doping., a facile approach to impart enhanced arsenic adsorption performance and easy magnetic separation capability to α- Fe_2O_3 nanoadsorbents. *J. Mater. Chem. A* **2013**, *1*, 830–836.
6. Akin, I.; Arslan, G.; Tor, A.; Ersoz, M.; Cengeloglu, Y. Arsenic(V) removal from underground water by magnetic nanoparticles synthesized from waste red mud. *J. Hazard. Mater.* **2012**, *235–236*, 62–68.
7. Wang, C.; Luo, H.; Zhang, Z.; Wu, Y.; Zhang, J.; Chen, S. Removal of As(III) and As(V) from aqueous solutions using nanoscale zero valent iron-reduced graphite oxide modified composites. *J. Hazard. Mater.* **2014**, *268*, 124–131.
8. Lenoble, V.; Bouras, O.; Deluchat, V.; Serpaud, B.; Bollinger, J.C. Arsenic adsorption onto pillared clays and iron oxides. *J. Colloid Interface Sci.* **2002**, *255*, 52–58.

Thank you for your attention!